

# NJL model of homogeneous neutral quark matter: Pseudoscalar diquark condensates revisited

H. Basler and M. Buballa

*Institut für Kernphysik, Technische Universität Darmstadt, Germany*

(Dated: April 20, 2010)

We use a Nambu-Jona Lasinio type model to investigate the phase diagram of dense quark matter under neutron star conditions in mean field approximation. The model contains selfconsistently determined quark masses and allows for diquark condensation in the scalar as well as in the pseudoscalar channel. The latter gives rise to the possibility of  $K^0$  condensation in the CFL phase. In agreement with earlier studies we find that this CFLK<sup>0</sup> phase covers large regions of the phase diagram and that the predominant part of this phase is fully gapped. We show, however, that there exists a region at very low temperatures where the CFLK<sup>0</sup> solutions become gapless, possibly indicating an instability towards anisotropic or inhomogeneous phases. The physical significance of solutions with pseudoscalar diquark condensates in the 2SC phase is discussed as well.

## I. INTRODUCTION

Matter at high density and low temperature is expected to be a color superconductor. (For reviews see, for example, Refs. [1–7]). At very high density, in the limit where QCD is weakly coupled, it is possible to investigate color superconductivity from first principles. From these studies [8, 9] we know that the ground state of three-flavor matter at asymptotically high density is the Color-Flavor Locked (CFL) phase [10], where quarks of all colors and flavors are paired in a homogeneous scalar ( $J^P = 0^+$ ) diquark condensate. Unfortunately, these analyses cannot directly be applied to describe the core of a neutron star, which is the most likely place for color superconducting quark matter to exist in nature. Although densities of several times nuclear matter density can be reached there, this is far from being asymptotic, and the weak-coupling expansion breaks down.

A second difficulty arises from the fact that, at these “moderate” densities, the strange quark mass cannot be neglected against the chemical potential. Moreover, in compact stars the system must be in beta equilibrium and electrically and color neutral. As a consequence, the Fermi momenta of the different quark flavors are unequal in the unpaired system, and their BCS pairing is only favored if the free-energy cost to adjust the Fermi surfaces is overcompensated by the pairing energy. It is therefore unclear whether quark matter under compact star conditions is color superconducting and, if so, which pairing pattern is most favored. Besides the CFL phase, the most prominent candidate is the 2SC phase [11, 12], where only up and down quarks are paired.

The stress imposed by the different Fermi momenta of the quarks in a diquark pair reduces the gap in the excitation spectrum. Eventually, the gap vanishes completely [13], and one obtains a “gapless color superconducting state”, e.g., the gapless 2SC (g2SC) phase [14, 15] or the gapless CFL (gCFL) phase [16, 17]. However, at least at low temperatures, these gapless phases suffer from chromomagnetic instabilities [18–20], indicating that they cannot be the true ground state of the sys-

tem. Possible alternatives are inhomogeneous phases, like mixed phases [21–23] or crystalline color superconducting phases [24–32].

Another way the CFL phase can react on the stress induced by the strange quark mass is to develop a  $K^0$  condensate. The resulting phase is called CFLK<sup>0</sup> phase. Since the  $K^0$  has strangeness +1 (opposite to a strange quark, which has strangeness −1), its condensation effectively reduces the strange quark content of the system. The  $K^0$  condensation was predicted first within an effective field theory approach based on the symmetry breaking pattern of the CFL phase [33–35]: The CFL condensates break the original  $SU(3)_{\text{color}} \times SU(3)_L \times SU(3)_R$  symmetry of QCD down to a residual  $SU(3)_{\text{color}+V}$  symmetry. As a consequence of the spontaneous breaking of chiral symmetry, there is an octet of pseudoscalar Goldstone bosons, which are massless in the chiral limit. Turning on finite quark masses, the Goldstone bosons remain rather light [36] whereas the strange quark mass acts as an effective strangeness chemical potential, which eventually leads to Bose condensation of the kaonic modes.

Since the kaon condensate reduces the stress in the diquark pairs, it is expected to shift the occurrence of gapless modes to lower chemical potentials. Within effective theories it was predicted that the first mode which becomes gapless is electrically charged [37, 38]. In Ref. [39] it was shown that all Meissner masses stay real in this phase, but nevertheless a weak instability towards the spontaneous generation of Goldstone-boson currents ( $p$ -wave kaon condensates) was found [40, 41]. At lower chemical potential a neutral mode could become gapless as well, leading to imaginary Meissner masses and stronger instabilities [39].

In order to decide, which of these various phases are realized under compact star conditions, detailed calculations are necessary. Unfortunately, as mentioned in the beginning, QCD calculations based on a weak-coupling expansion are not applicable at moderate densities. In this situation the most promising development is probably the Dyson-Schwinger approach, which has been successfully extended to describe color superconducting

quark matter [42–45]. However, because of the complexity of this method it is difficult to apply it to the calculation of equations of state or phase diagrams. So far, the most complete investigations of quark matter under compact star conditions have therefore been performed within models. Although model calculations have only limited predictive power, they can deal as explorative studies and may give valuable hints about possible interesting scenarios or problems. Among these models for color superconducting quark matter, the most prominent ones are models of the Nambu–Jona-Lasinio (NJL) type, because they allow for a simultaneous and selfconsistent treatment of the various condensates. Besides the diquark condensates this also includes the chiral (quark-antiquark) condensates, which determine the dynamical quark masses.

Phase diagrams for homogeneous electrically and color neutral quark matter in NJL-type models have been calculated in Refs. [46–49]. Both, diquark and quark antiquark condensates, were included, but the authors neglected the possibility of Goldstone boson condensation. A rich phase structure was found, including large areas of gapless color superconducting phases. Unfortunately, the details strongly depend on the model parameters.

For the description of CFL+Goldstone boson condensed phases in NJL-type models one has to take into account pseudoscalar diquark condensates [50, 51]. In the chiral limit the Goldstone bosons connect the continuous set of degenerate ground states which are related to each other by axial SU(3) transformations,

$$q \rightarrow \exp\left(i\theta_a \frac{\tau_a}{2} \gamma_5\right) q, \quad (1)$$

where  $q$  is a quark field and  $\tau_a$ ,  $a = 1, \dots, 8$ , are the Gell-Mann matrices in flavor space. Under these transformations the scalar diquark condensates of the CFL phase are partially rotated into pseudoscalar ones. In particular, the  $K^0$  condensation is marked by the formation of pseudoscalar condensates which correspond to Eq. (1) with  $a = 6, 7$ , whereas charged pion or charged kaon condensates correspond to  $a = 1, 2$  or  $a = 4, 5$ , respectively.

In Ref. [52], Warringa extended the NJL-model studies of Ref. [46] in this direction. Using the same model and the same parameters but additionally allowing for pseudoscalar condensates, he found that large parts of the CFL and gCFL phases are replaced by the CFLK<sup>0</sup> phase. Moreover, Warringa reported that the CFLK<sup>0</sup> solutions contain no gapless modes, suggesting that no instability problems occur. On the other hand he found that, below a certain threshold in the chemical potential, the electric charge chemical potential at  $T = 0$  is nonzero in this phase. This would mean that there is a nonvanishing electron density, which is not allowed in the fully gapped neutral CFLK<sup>0</sup> phase at zero temperature.

The main motivation of our present study was to resolve this puzzle. To that end we use the same model as in Ref. [52] and carefully analyze the phase diagram and the excitation spectra. As we will see, to a large extent our results are in good agreement with Ref. [52]. The

main difference is that we find a region where the CFLK<sup>0</sup> phase is gapless. However, this region is restricted to extremely low temperatures,  $T \ll 10$  keV. We will also analyze the so-called p2SC phase, a 2SC-like phase with pseudoscalar condensates, which was found in Ref. [52] but has no obvious physical interpretation.

The remaining part of this paper is organized as follows. In Sec. II we introduce the model and briefly summarize how the thermodynamic potential is obtained. After that, in Sec. III, we discuss the resulting phase structure. We begin with a short overview in Sec. III A and then perform a detailed analysis of the most interesting features. Finally, in Sec. IV, our results are summarized.

## II. MODEL

### A. Lagrangian

We use the same NJL-type model as in Refs. [46, 52]. The Lagrangian reads

$$\mathcal{L} = \bar{q}(i\cancel{\partial} - \hat{m} + \gamma_0 \hat{\mu})q + \mathcal{L}_{\bar{q}q} + \mathcal{L}_{qq} + \mathcal{L}_6, \quad (2)$$

where  $q$  is a quark field with three color ( $r, g, b$ ) and three flavor ( $u, d, s$ ) degrees of freedom.  $\hat{m}$  is the diagonal mass matrix  $\hat{m} = \text{diag}_f(m_u, m_d, m_s)$ .

The diagonal matrix  $\hat{\mu}$  contains the quark chemical potentials. As motivated in the Introduction, we are interested in the electrically and color neutral ground state in beta equilibrium. We then have four different conserved charges: the total quark number, the electric charge and two color charges. According to the corresponding charge densities  $n$ ,  $n_Q$ ,  $n_3 = n_r - n_g$  and  $n_8 = (n_r + n_g - 2n_b)/\sqrt{3}$ , we thus have four independent chemical potentials  $\mu$ ,  $\mu_3$ ,  $\mu_8$ , and  $\mu_Q$ . So  $\hat{\mu}$  takes the form

$$\hat{\mu} = \mu + \mu_Q Q + \mu_3 \lambda_3 + \mu_8 \lambda_8, \quad (3)$$

with  $Q = \text{diag}_f(2/3, -1/3, -1/3)$  and the Gell-Mann matrices  $\lambda_3$  and  $\lambda_8$  in color space.

The other terms in Eq. (2) describe the interaction.

$$\mathcal{L}_{\bar{q}q} = G \sum_{a=0}^8 \left[ (\bar{q} \tau_a q)^2 + (\bar{q} i \gamma_5 \tau_a q)^2 \right] \quad (4)$$

is a four-point interaction in the quark-antiquark channel, while

$$\begin{aligned} \mathcal{L}_{qq} = H \sum_{A,B=2,5,7} & \left[ (\bar{q} i \gamma_5 \tau_A \lambda_B C \bar{q}^T) (q^T C i \gamma_5 \tau_A \lambda_B q) \right. \\ & \left. + (\bar{q} \tau_A \lambda_B C \bar{q}^T) (q^T C \tau_A \lambda_B q) \right], \end{aligned} \quad (5)$$

is a four-point interaction in the quark-quark channel.  $G$  and  $H$  are dimensionful coupling constants. In our notation  $\lambda_a$  and  $\tau_a$  are the Gell-Mann matrices acting

	$\Delta_{22}^{(s)}$	$\Delta_{55}^{(s)}$	$\Delta_{77}^{(s)}$	$\Delta_{25}^{(p)}$	$\Delta_{52}^{(p)}$	$\Delta_{27}^{(p)}$	$\Delta_{72}^{(p)}$	$\Delta_{57}^{(p)}$	$\Delta_{75}^{(p)}$
NQ	-	-	-	-	-	-	-	-	-
2SC	×	-	-	-	-	-	-	-	-
uSC	×	×	-	-	-	-	-	-	-
p2SC	×	-	-	×	-	-	-	-	-
CFL	×	×	×	-	-	-	-	-	-
CFLK <sup>0</sup>	×	×	×	×	×	-	-	-	-
CFLK <sup>±</sup>	×	×	×	-	-	×	×	-	-
CFL $\pi^{\pm}$	×	×	×	-	-	-	-	×	×

TABLE I: The phases investigated in this article.  $\times$  marks the presence of the condensates while  $-$  means that the condensate vanishes.

in color space and in flavor space, respectively, where  $\tau_0 = \sqrt{2/3} \mathbf{1}_f$ .  $C$  denotes the charge conjugation matrix  $C = i\gamma^2\gamma^0$ .

Both,  $\mathcal{L}_{\bar{q}q}$  and  $\mathcal{L}_{qq}$ , consist of a scalar part (first term on the r.h.s.) and a pseudoscalar part (second term on the r.h.s.) and are invariant under flavor  $U(3)_L \times U(3)_R$  transformations. In order to break the  $U(1)$  axial symmetry, we include a six-point ('t Hooft) interaction term [53]

$$\mathcal{L}_6 = -K \{ \det_f [\bar{q}(1 + \gamma_5)q] + \det_f [\bar{q}(1 - \gamma_5)q] \}, \quad (6)$$

with coupling constant  $K$ .

## B. Phases and condensates

We introduce the following scalar and pseudoscalar diquark condensates<sup>1</sup>

$$\Delta_{AB}^{(s)} = -2H \langle q^T C \gamma_5 \tau_A \lambda_B q \rangle, \quad (7)$$

$$\Delta_{AB}^{(p)} = -2H \langle q^T C \tau_A \lambda_B q \rangle. \quad (8)$$

Depending on which of these diquark condensates take nonzero values, we can distinguish various color superconducting phases. The phases which have been investigated in this article are summarized in Table I. For instance, in the simplest possible color superconducting phase, the 2SC phase, only the  $\Delta_{22}^{(s)}$  condensate is present. In this phase only red and green up and down quarks form Cooper pairs while the strange and all blue quarks remain unpaired (see Table II). In the uSC phase [54]  $\Delta_{22}^{(s)}$  and  $\Delta_{55}^{(s)}$  are nonzero. Here red and blue up and strange quarks are paired, in addition to the pairs which are already present in the 2SC phase.

The most symmetric phase is the CFL phase, where  $\Delta_{22}^{(s)}$ ,  $\Delta_{55}^{(s)}$  and  $\Delta_{77}^{(s)}$  are non-zero, so that all quark flavors and colors are paired in a scalar condensate. As in QCD, the presence of these condensates breaks the original  $SU(3)_{\text{color}} \times SU(3)_L \times SU(3)_R$  of the model down to  $SU(3)_{\text{color}+V}$ . Among others, this gives rise to an octet of pseudoscalar Goldstone bosons (see Refs. [55–58] for the NJL-model description of these Goldstone bosons). The condensation of some of these Goldstone bosons is then marked by the appearance of nonvanishing pseudoscalar condensates. For instance, applying the transformation of Eq. (1) in the  $K^0$  channel ( $a = 6, 7$ ) on the scalar condensates of the CFL phase gives rise to the pseudoscalar condensates  $\Delta_{25}^{(p)}$  and  $\Delta_{52}^{(p)}$ . Similarly, in the CFLK<sup>±</sup> phase the condensates  $\Delta_{27}^{(p)}$  and  $\Delta_{72}^{(p)}$ , and in the CFL $\pi^{\pm}$  phase the condensates  $\Delta_{57}^{(p)}$  and  $\Delta_{75}^{(p)}$  appear.

In the 2SC phase, there are no pseudoscalar Goldstone bosons. Nevertheless, it was found in Ref. [52] that in some region of the phase diagram a so-called p2SC phase is favored, where a pseudoscalar condensate is present in addition to  $\Delta_{22}^{(s)}$ . Therefore we will consider this possibility as well.

On the other hand, we will not consider other combinations of scalar diquark condensates, i.e., the dSC phase ( $\Delta_{22}^{(s)} \neq 0$  and  $\Delta_{77}^{(s)} \neq 0$ ), the sSC phase ( $\Delta_{55}^{(s)} \neq 0$  and  $\Delta_{77}^{(s)} \neq 0$ ), the 2SC<sub>us</sub> phase ( $\Delta_{55}^{(s)} \neq 0$ ), or the 2SC<sub>ds</sub> phase ( $\Delta_{77}^{(s)} \neq 0$ ). These possibilities were taken into account in Refs. [46] and [52], but were not found to be realized in the phase diagram. So we do not expect them to play a role.

In addition to the diquark condensates, we also introduce scalar antiquark-quark condensates

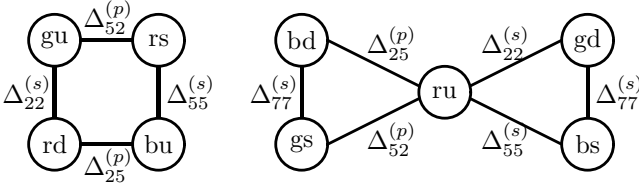
$$\phi_f = \langle \bar{q}_f q_f \rangle, \quad f \in \{u, d, s\}, \quad (9)$$

which are responsible for spontaneous chiral symmetry breaking at low temperatures and densities. Since chiral symmetry is explicitly broken by the mass matrix  $\hat{m}$ , this does not lead to new phases in a strict sense. However, it gives rise to dynamical “constituent” quark masses (see Eq. (17) below) which can be considerably larger than the bare masses contained in  $\hat{m}$ .

Expecting that the condensation of pions and kaons outside the color superconducting phase does not occur, we neglect condensates of the form  $\langle \bar{q} i \gamma_5 \tau_a q \rangle$ . In principle, such condensates should be present in the CFL+Goldstone boson phases where they break no additional symmetry. However, following Ref. [52], we neglect them there as well, expecting that their effect is small. Eventually, this should be checked.

At the end of this section, we would like to add a few more details about the CFLK<sup>0</sup> phase and compare them with the more familiar CFL phase. Later on, this will be useful for the interpretation of the results. In Fig. 1 we show the color-flavor structure of the CFLK<sup>0</sup> pairing. This pattern follows directly from Tables I and II. If we switch off the pseudoscalar condensates, we arrive

<sup>1</sup> For the comparison with Ref. [52] it is important to note that we use the notation of Ref. [50] for the diquark condensates,  $\Delta_{\text{flavor}, \text{color}}$ , while in Ref. [52] they are denoted in the opposite way,  $\Delta_{\text{color}, \text{flavor}}$ .

FIG. 1: Pairing pattern in the CFLK<sup>0</sup> phase.

at the CFL pairing pattern. There the quarks can be grouped into four subsets, which are not connected to each other by the pairing. In the CFLK<sup>0</sup> phase, the pseudoscalar condensates give rise to additional connections, so that only two unconnected subsets remain. The smaller one consists of four pairs, connecting four different quark species, the larger one contains six pairs, which connect five quark species.

In Table II we have also listed the eigenvalues of the “rotated” electric charges

$$\tilde{Q} = Q - \frac{1}{2}\lambda_3 - \frac{1}{2\sqrt{3}}\lambda_8 \quad (10)$$

for both constituents of each pair. For the CFL phase it is well known that the ground state is  $\tilde{Q}$  neutral [10, 59]. This follows from the fact that all quarks are paired and in each pair the sum  $\tilde{Q}_1 + \tilde{Q}_2$  vanishes. Obviously, the same is true for the CFLK<sup>0</sup> phase. An important consequence is that, at  $T = 0$ , in both phases color neutral quark matter is automatically electrically neutral. Hence, no electrons are admitted in neutral matter, i.e.,  $\mu_Q = 0$  [60, 61].

gap parameter	diquark pair	$\tilde{Q}_1$	$\tilde{Q}_2$
$\Delta_{22}^{(s)}$	$ru - gd$	0	0
	$gu - rd$	1	-1
$\Delta_{55}^{(s)}$	$ru - bs$	0	0
	$bu - rs$	1	-1
$\Delta_{77}^{(s)}$	$gd - bs$	0	0
	$bd - gs$	0	0
$\Delta_{25}^{(p)}$	$ru - bd$	0	0
	$bu - rd$	1	-1
$\Delta_{52}^{(p)}$	$ru - gs$	0	0
	$gu - rs$	1	-1

TABLE II: Gap parameters, color-flavor structure of the corresponding diquark pairs and  $\tilde{Q}$  charges of the constituents. The list is restricted to those condensates which are realized in the phase diagrams of Sect. III.

While all pairs listed in Table II are  $\tilde{Q}$  neutral in total, we can distinguish two cases: either both quarks carry zero  $\tilde{Q}$  charge (like in the  $ru - gd$  pair) or the quarks carry the  $\tilde{Q}$  charges  $\pm 1$  (like in the  $gu - rd$  pair). Comparing this with Fig. 1, we see that the two unconnected groups in the pairing pattern of the CFLK<sup>0</sup> phase just correspond to these two cases.

### C. Thermodynamic potential

In order to decide, which phase is favored at given temperature and chemical potential, we calculate the thermodynamic potential per volume,

$$\Omega = \frac{T}{V} \ln \mathcal{Z}, \quad (11)$$

where  $\mathcal{Z}$  is the grand partition function. Besides the quarks we consider the presence of noninteracting leptons,

$$\Omega = \Omega_q + \Omega_l, \quad (12)$$

where  $\Omega_l = \Omega_e + \Omega_\mu$  is the sum of the ideal gas contributions of electrons and muons. For the quark part  $\Omega_q$  we restrict ourselves to the mean-field approximation and proceed in the same way as described in Refs. [46, 52, 62]. Therefore, we only summarize the main steps here and refer to these papers for further details.

Linearizing the interaction around the condensates defined above and introducing Nambu-Gorkov bispinors,

$$\Psi = \frac{1}{\sqrt{2}} \begin{pmatrix} q \\ C\bar{q}^T \end{pmatrix}, \quad (13)$$

we obtain the mean-field Lagrangian

$$\mathcal{L}^{\text{MF}} = \bar{\Psi} S^{-1} \Psi - \mathcal{V} \quad (14)$$

where

$$\begin{aligned} \mathcal{V} = & 2G(\phi_u^2 + \phi_d^2 + \phi_s^2) - 4K\phi_u\phi_d\phi_s \\ & + \frac{1}{4H} \sum_{A,B=2,5,7} \left[ \left( \Delta_{AB}^{(s)} \right)^2 + \left( \Delta_{AB}^{(p)} \right)^2 \right] \end{aligned} \quad (15)$$

is a field-independent potential density, and  $S^{-1}$  is the inverse dressed propagator, which in momentum space is given by

$$S^{-1}(p) = \begin{pmatrix} \not{p} + \hat{\mu}\gamma^0 - \hat{M} & \sum_{A,B} \left( \Delta_{AB}^{(s)} \gamma_5 \tau_A \lambda_B + \Delta_{AB}^{(p)} \tau_A \lambda_B \right) \\ \sum_{A,B} \left( -\Delta_{AB}^{(s)} \gamma_5 \tau_A \lambda_B + \Delta_{AB}^{(p)} \tau_A \lambda_B \right) & \not{p} - \hat{\mu}\gamma^0 - \hat{M} \end{pmatrix}. \quad (16)$$

It is a  $72 \times 72$  matrix, corresponding to three color, three flavor, four Dirac, and two Nambu-Gorkov degrees of freedom.  $\hat{M}$  is the diagonal matrix of the constituent quark masses with the components

$$M_a = m_a - 4G\phi_a + 2K\phi_b\phi_c, \quad (17)$$

where  $(a, b, c)$  is any permutation of  $(u, d, s)$ .

The quark part of the thermodynamic potential in mean-field approximation is then given by

$$\Omega_q(T, \{\mu_i\}) = -T \sum_n \int \frac{d^3p}{(2\pi)^3} \frac{1}{2} \text{Tr} \ln \left( \frac{S^{-1}(i\omega_n, \vec{p})}{T} \right) + \mathcal{V}. \quad (18)$$

The  $\text{Tr} \ln$  is evaluated by determination of the 72 eigenvalues of  $S^{-1}$ . Making use of a two-fold spin degeneracy, the problem can be reduced to calculating the eigenvalues of a  $36 \times 36$  matrix [46]. This matrix can be transformed further into block-diagonal form, where the number and size of the blocks depend on the pairing pattern. For instance, in the CFL phase we get one  $12 \times 12$  block and six  $4 \times 4$  blocks, whereas in the CFL + Goldstone phases we have one  $20 \times 20$  block and two  $8 \times 8$  blocks. The different blocks can be attributed to quasiparticle excitations with different quantum numbers. For instance, in the CFLK<sup>0</sup> phase the  $20 \times 20$  block corresponds to quasiparticles with  $\tilde{Q} = 0$  whereas the two  $8 \times 8$  blocks correspond to quasiparticles with  $\tilde{Q} = +1$  or  $\tilde{Q} = -1$ , respectively.

The resulting eigenvalues appear in the form  $i\omega_n - \epsilon_j(\vec{p})$ , where  $\epsilon_j(\vec{p})$  are the energy-independent eigenvalues of the Matrix  $\mathcal{M} = i\omega_n - \gamma^0 S^{-1}$  and correspond to the dispersion relations of the quasiparticle modes. This allows for an analytic evaluation of the Matsubara sum, and we finally get

$$\Omega_q = - \int \frac{d^3p}{(2\pi)^3} \sum_{j=1}^{18} \left( |\epsilon_j| + 2 T \ln \left( 1 + e^{-\frac{|\epsilon_j|}{T}} \right) \right) + \mathcal{V}. \quad (19)$$

Here we have used the fact that the eigenvalues come in pairs  $(\epsilon_j, -\epsilon_j)$ , so that we can restrict the sum, e.g., to the 18 positive eigenvalues, introducing an extra factor of 2. The integral is divergent and will be regularized by a sharp three-momentum cutoff  $\Lambda$ .

In order to find the most stable solution, we have to minimize the thermodynamic potential with respect to the various diquark and quark-antiquark condensates, i.e., we have to solve the gap equations

$$\frac{\partial \Omega}{\partial \phi_f} = \frac{\partial \Omega}{\partial \Delta_{AB}^{(s)}} = \frac{\partial \Omega}{\partial \Delta_{AB}^{(p)}} = 0, \quad (20)$$

with  $f \in \{u, d, s\}$  and  $A, B \in \{2, 5, 7\}$ . In addition, since we are interested in quark matter under compact star conditions, our solution must fulfill the neutrality constraints

$$n_Q = -\frac{\partial \Omega}{\partial \mu_Q} = 0, \quad n_3 = -\frac{\partial \Omega}{\partial \mu_3} = 0, \quad n_8 = -\frac{\partial \Omega}{\partial \mu_8} = 0. \quad (21)$$

Eqs. (20) and (21) form a set of coupled nonlinear equations which determines the values of the condensates and the chemical potentials  $\mu_Q$ ,  $\mu_3$ , and  $\mu_8$  for any given quark chemical potential  $\mu$  and temperature  $T$ . For the evaluation of the derivatives in these equations we follow Ref. [52], making use of the diagonalized form of the propagator. Finally, we checked for each solution that the off-diagonal color densities vanish as well (cf. Ref. [63] and the discussion in Sec. III D).

#### D. Model parameters

For the numerical calculations, we adopt the parameter values of Ref. [64],

$$\begin{aligned} m_u = m_d &= 5.5 \text{ MeV}, \\ m_s &= 140.7 \text{ MeV}, \\ G &= 1.835/\Lambda^2, \\ K &= 12.36/\Lambda^5, \\ \Lambda &= 602.3 \text{ MeV}, \end{aligned} \quad (22)$$

which have been fixed by fitting the vacuum values of the pseudoscalar meson masses and the pion decay constant. The same parameter values have also been used in Refs. [46] and [52]. For the diquark coupling strength, which cannot be fixed in this way, we follow Ref. [46] and take two different values, namely  $H = 3/4 G$ , which can be motivated by the Fierz transformation of a one-gluon exchange, or  $H = G$ .

For the leptonic part, we consider massless electrons and muons with mass 105.66 MeV. Here we differ slightly from Refs. [46, 52] where a physical electron mass  $m_e = 511 \text{ keV}$  was taken. Obviously this is negligible in most cases, but it could play a role at  $T, |\mu_Q| \lesssim m_e$ . As we will see, this situation is just realized in the vicinity of the threshold of the gapless CFLK<sup>0</sup> phase. We will comment on this at the end of Sec. III B.

### III. RESULTS

In this section we discuss the phase structure of the model. We begin with a brief overview and then analyze the most interesting features in more detail.

#### A. Phase diagram

As discussed in Sec. II C, we obtain the phase diagram in the  $\mu - T$  - plane, by minimizing the thermodynamic potential at every point of that plane with respect to the various condensates, taking into account the constraints of beta equilibrium and local electric and color neutrality. We thereby consider all phases which are listed in Tab. I. We recall that, while these phases are distinguished by their contents of nonvanishing diquark condensates, the chiral quark-antiquark condensates  $\phi_f$  are

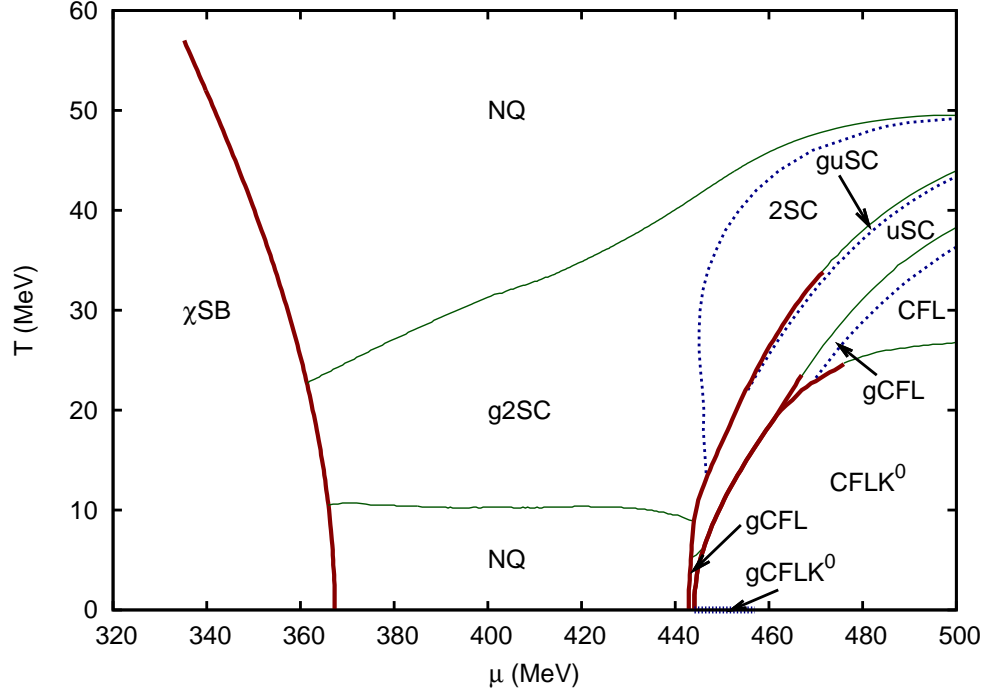


FIG. 2: The phase diagram of charge and color neutral quark matter for “intermediate diquark coupling”,  $H = 3/4 G$ . Red thick solid lines denote first-order phase transitions, green thin solid lines second-order phase transitions, the blue dotted lines mark the (dis)appearance of the gap in the excitation spectrum.

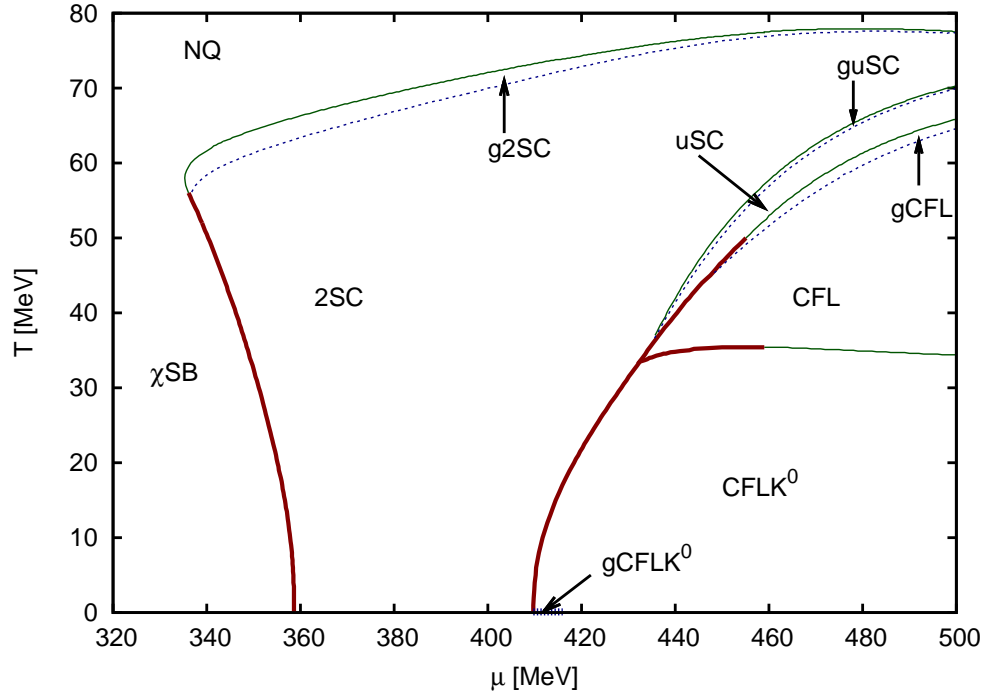


FIG. 3: The same as Fig. 2, but for “strong diquark coupling”,  $H = G$ .

selfconsistently determined as well. Strictly speaking, since chiral symmetry is explicitly broken in the model, this is not related to additional phases. However, follow-

ing Ref. [46], we label regions where  $\phi_u$  and  $\phi_d$  are large by ‘ $\chi_{SB}$ ’ and regions where these condensates are small by ‘NQ’. Both regimes are not necessarily separated by

a phase boundary.

The resulting phase diagrams are displayed in Figs. 2 and 3. In Fig. 2 the diquark coupling constant was chosen to be  $H = 3/4 G$ . To a large extent our results agree qualitatively and quantitatively with those of Warringa, who has calculated the phase diagram within the same model for the same parameters [52]: Compared with Ref. [46], where only scalar diquark condensates have been taken into account, the main effect of considering pseudoscalar condensates is the existence of a CFLK<sup>0</sup> phase, which replaces most of the (g)CFL phase at temperatures below  $\approx 25$  MeV. A second effect, which was reported in Ref. [52], is the emergence of a p2SC phase, i.e., a two-flavor color superconductor with an additional pseudoscalar condensate, replacing a part of the 2SC phase in the region around  $\mu = 460$  MeV and  $T = 30$  MeV. Although this result is confirmed by our calculations (see Fig. 11 below), we have not indicated the p2SC phase in the phase diagram, because it is most likely a model artifact. This will be discussed in Sec. IIID.

While most of our results agree with Ref. [52], there are basically two exceptions: First, we find that the CFLK<sup>0</sup> phase becomes gapless at extremely low temperatures and  $\mu < 457.2$  MeV, whereas it was claimed in Ref. [52] that it is always gapped. We discuss this in more details in Sec. IIIB. The second difference concerns the phase structure between the normal phase (NQ) and the CFLK<sup>0</sup> phase at low temperatures. In contrast to the results of Ref. [52] we do not find a uSC phase down to zero temperature. Instead we find a situation more like in Ref. [46], where at temperatures lower than  $\approx 7$  MeV a gCFL phase is realized. This will be discussed in Sec. IIIC.

In Fig. 3 we show the phase diagram for the diquark coupling constant  $H = G$ . This case was not studied in Ref. [52]. However, it was investigated in Ref. [46], considering scalar diquark condensates only. By comparing that phase diagram with Fig. 3, we see that the effects of the pseudoscalar condensates are qualitatively similar to the previous case: A major part of the CFL phase is replaced by the CFLK<sup>0</sup> phase, which now persists up to temperatures of about 35 MeV. At very low temperatures and  $\mu < 415.6$  MeV the CFLK<sup>0</sup> phase is gapless. Numerically, we also find again a p2SC phase, which replaces the 2SC phase in some region. However, as mentioned before, we believe that this is a model artifact (see Sec. IIID) and do not indicate this phase in the phase diagram.

## B. The gapless CFLK<sup>0</sup> phase

Both, in Fig. 2 and Fig. 3, there is a gapless CFLK<sup>0</sup> phase at very low temperatures below a certain value of  $\mu$ . For the case  $H = 3/4 G$  this is illustrated in Fig. 4. In the upper part, the gap in the quasiparticle excitation spectrum is displayed as a function of  $\mu$ . In gen-

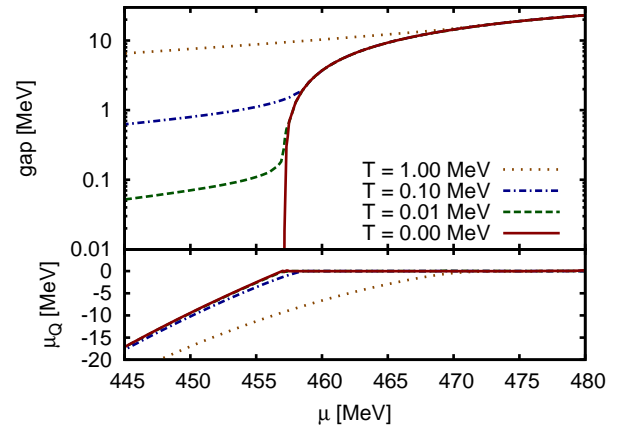


FIG. 4: The gap in the excitation spectrum and the electric charge chemical potential  $\mu_Q$  in the (g)CFLK<sup>0</sup> phase as functions of the chemical potential for  $H = 3/4 G$  and various temperatures.

eral, the gaps are nonzero at higher chemical potentials and decrease with decreasing chemical potential. At zero temperature (red solid line) it eventually goes to zero at  $\mu = 457.2$  MeV, so that there is indeed a gapless phase below that threshold.

It turns out, however, that this behavior is extremely sensitive to the temperature. At  $T = 1$  MeV (yellow dotted line), which is often a very good approximation to zero temperature, the gap stays of the order of several MeV and there is no indication for a nearby gapless phase. At lower temperatures, the gap first follows the  $T = 0$  behavior but then levels off and stays finite. Even at  $T = 0.01$  MeV (green dash-dotted line), the gapless phase is not reached. This seems to suggest, that the gapless CFLK<sup>0</sup> phase only exists at zero temperature.<sup>2</sup>

This picture is corroborated by Fig. 5, where the excitation gaps are displayed as functions of temperature at fixed chemical potential. For  $\mu = 450$  MeV the numerical values (which are explicitly indicated by the points) show an almost perfect linear behavior, so that, within numerical accuracy, the CFLK<sup>0</sup> phase becomes gapless exactly at  $T = 0$ . For comparison, we also show the results for  $\mu = 460$  MeV. In this case the gap levels off and stays finite at  $T = 0$ .

In the lower part of Fig. 4 the electric charge chemical potential  $\mu_Q$  is plotted as a function of  $\mu$  for the same temperatures as the excitations gaps shown in the upper part. At zero temperature, as explained in Sect. IIB,

<sup>2</sup> Note that this has nothing to do with the fact that only at  $T = 0$  the transition from a gapped to a gapless phase corresponds to a real phase transition with a well defined order parameter. Here we identify the gapless regimes by inspecting the gaps in the excitation spectrum, which can be done at any temperature. As one can see in Figs. 2 and 3, other gapless phases defined in this way do exist at  $T > 0$ , see also Refs. [46, 47, 49, 52].

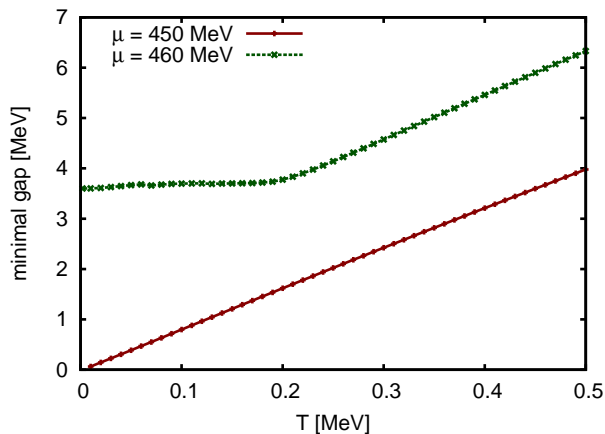


FIG. 5: The gap in the excitations spectrum as function of the temperature for  $H = 3/4 G$  and two different values of  $\mu$ .

$\mu_Q$  is an order parameter, which vanishes in the gapped phase and is nonzero in the gapless phase. This is no longer true at  $T > 0$  where  $\mu_Q$  is always nonzero. Nevertheless, one might expect that at low enough temperatures  $\mu_Q$  is very small in the gapped regime, so that larger deviations from zero signal a gapless phase. It turns out, however, that this is not the case. For  $T = 1$  MeV, 0.1 MeV, or 0.01 MeV,  $\mu_Q$  exhibits a threshold-like behavior, although we do not enter a gapless regime. When we compare these “thresholds” with the upper part of Fig. 4, we see that they more or less coincide with the positions where the excitation gaps start deviating from the  $T = 0$  gaps. In fact, as we will discuss, the mechanism which keeps the excitation gaps finite at  $T > 0$  is closely related to the rise of  $-\mu_Q$ .

To understand this, we take a more detailed look at the low-energy quasiparticle excitation spectra and thereby compare the gCFLK<sup>0</sup> phase with the more familiar gCFL phase. A similar comparison has been performed earlier in Ref. [51], but restricted to zero temperature and to the gapped or the threshold to the gapless regime. Here we go deeper into the gapless regime and also discuss temperature effects.

In Fig. 6 the quasiparticle spectra at  $\mu = 450$  MeV are shown for  $T = 0$  (left) and  $T = 5$  MeV (right). The two lower panels correspond to the (g)CFLK<sup>0</sup> phase, while in the two upper panels the analogous gCFL solutions are shown, which are obtained if the pseudoscalar diquark condensates are not taken into account. Since  $\tilde{Q}$  is a conserved quantum number in both cases, the quasiparticle excitations carry a definite  $\tilde{Q}$  charge. These  $\tilde{Q}$  charges, which can be 0, +1, or -1, are indicated in Fig. 6 as well.

Let us begin with the discussion of the gCFL solutions. At  $T = 0$  (upper left panel) there are two gapless modes. One of them vanishes at two different momenta, separated by a “blocking region” of about 100 MeV. This mode has  $\tilde{Q} = 0$  and can be identified with a  $bd$ -particle  $gs$ -hole mode. In addition, there is another gapless mode (which has  $\tilde{Q} = +1$  and is a  $bu$ -particle  $rs$ -hole mode),

which seems to vanish just at its minimum. On a much smaller scale one finds that this is not exactly true, but there is a finite blocking region as well. It is, however, very small and therefore not visible in the figure. (For the analogous mode in the gCFLK<sup>0</sup> phase, this is discussed in Fig. 8.)

This behavior is well known and has been explained in Ref. [17]. It was shown that at  $T = 0$  both modes, the  $bd - gs$  mode and the  $bu - rs$  mode, become gapless at the same critical chemical potential but behave rather differently when  $\mu$  is further decreased: In the  $bu - rs$  mode, the pair breaking leads to unpaired  $bu$  quarks in the blocking region, which carry positive  $\tilde{Q}$  charge. Color neutral quark matter is therefore positively charged and must be neutralized by electrons. This requires  $\mu_Q < 0$ , which, in turn, reduces the stress in the  $bu - rs$  pairs and keeps the blocking region very small. For the  $bd - gs$  mode, on the other hand, there is no such mechanism because both quarks have  $\tilde{Q} = 0$ . As a consequence, the blocking region becomes much wider.

When we increase the temperature to 5 MeV, as shown in the upper right panel of Fig. 6, the  $bd - gs$  mode remains gapless, whereas the  $bu - rs$  mode receives a considerable gap. A detailed numerical analysis reveals that this mode behaves in a similar way as the lowest CFLK<sup>0</sup> mode in Fig. 5. In particular, it becomes already gapped if the temperature is increased only slightly above zero. This is naturally explained by Fermi smearing effects. In fact, it is a well-known phenomenon that modes which are gapless at  $T = 0$  can become gapped above a certain temperature [15]. In the present case, where the blocking region at  $T = 0$  is very small, it is plausible that the gapless regime is restricted to very small temperatures. On the other hand, since the size of the blocking region at  $T = 0$  is not exactly equal to zero, the “critical” temperature should be nonzero as well. It is, however, too small to be determined numerically.

We now compare these results with the spectra in the (g)CFLK<sup>0</sup> phase, which are displayed in the lower part of Fig. 6. At  $T = 0$  (left), there is again a marginally gapless  $\tilde{Q} = +1$  mode with a tiny blocking region around its minimum (cf. Fig. 8 below). The essential difference to the gCFL phase is, however, that the gCFLK<sup>0</sup> phase contains no second gapless mode, in which  $\tilde{Q} = 0$  quarks are paired. The size of the gapless regime is therefore determined by the lowest  $\tilde{Q} = +1$  mode. The latter can be seen as a “close relative” of the  $bu - rs$  in the gCFL phase. In the (g)CFLK<sup>0</sup> phase a complication arises due to the fact that not only two, but four quark species mix in the  $\tilde{Q} = \pm 1$  quasiparticle modes (cf. Fig. 1). The result of the numerical diagonalization is shown in Fig. 7 where the composition of the gapless mode is displayed as a function of the three-momentum. In agreement with Ref. [51], we find that the gapless mode is mainly a mixture of  $bu$  and  $gu$  particles with  $rs$  holes. The blocking of the  $rs$  quarks in the gapless regime then leads again to a surplus of positive  $\tilde{Q}$  charge, which forces the blocking region to stay very small. As a consequence, this mode



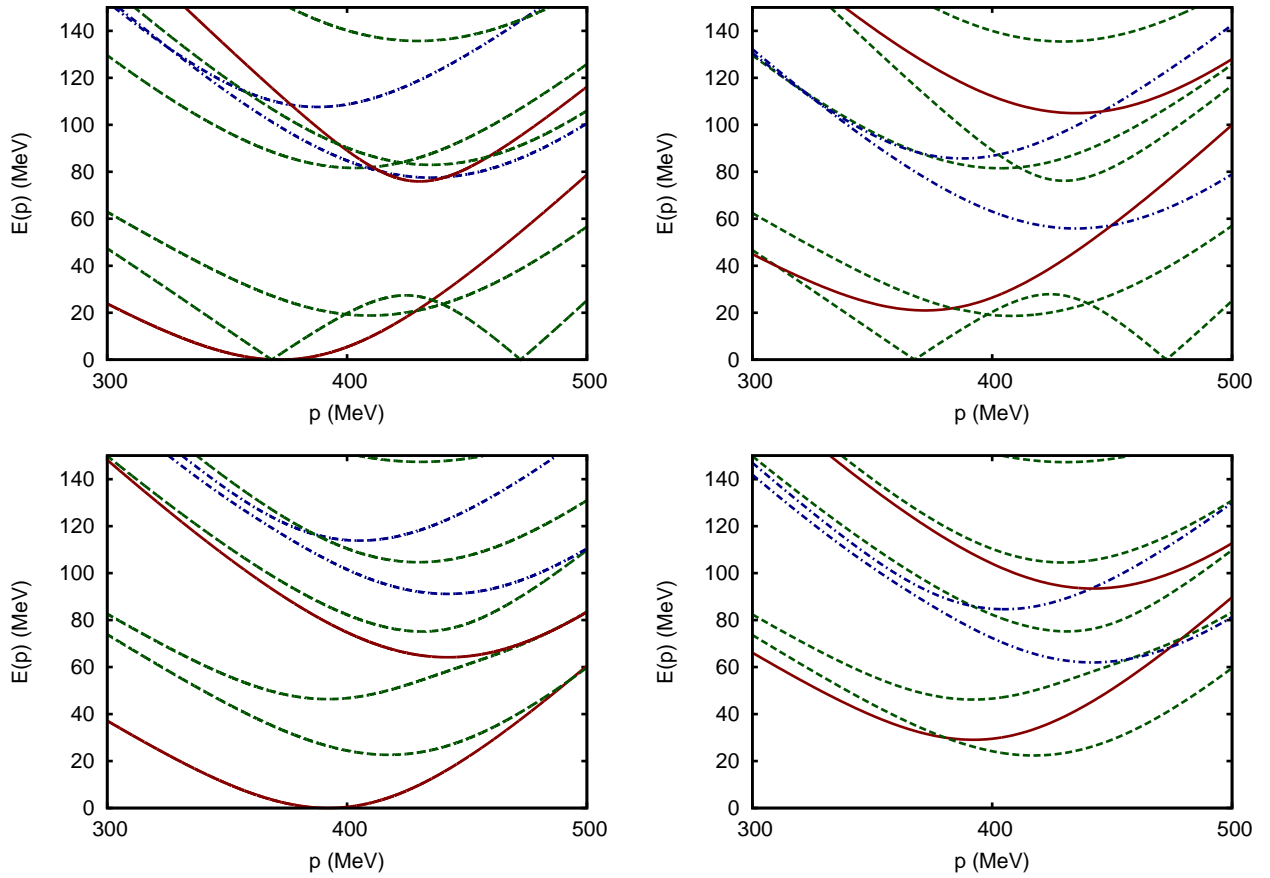


FIG. 6: Quasiparticle dispersion relations in the gCFL phase (top) and in the (g)CFLK<sup>0</sup> phase (bottom) at  $\mu = 450$  MeV and  $T = 0$  (left) or  $T = 5$  MeV (right);  $H = 3/4 G$ . The different line types correspond to modes with different  $\tilde{Q}$  charges:  $\tilde{Q} = +1$  (red solid lines),  $\tilde{Q} = 0$  (green dashed lines),  $\tilde{Q} = -1$  (blue dash-dotted lines).

and, hence the CFLK<sup>0</sup> phase is gapless only at very low temperatures.

Our results at  $T = 0$  are in qualitative agreement with the effective field theory prediction that the first gapless mode in the CFLK<sup>0</sup> phase is electrically charged [37–39]. According to these works, there could be a second phase transition at lower chemical potential, where a neutral mode becomes gapless as well. In fact, we found such solutions in some region of the phase diagram, but they were never favored. We will come back to this point in Sec. III C.

Concerning the electrically charged gapless modes, we found some quantitative differences to the effective theory results. In Refs. [37, 38] it was predicted that the charged mode becomes gapless at  $M_s^2/(2\mu) \approx 4/3 \Delta$ , where  $\Delta$  is the CFL gap in the chiral limit. Comparing this with the corresponding threshold in the CFL phase,  $M_s^2/(2\mu) \approx \Delta$ , and assuming that the strange quark mass is the same in both cases, this means that the critical chemical potential for entering the gapless regime is 25% lower in the kaon condensed phase. In Ref. [51] it was found that the effect is somewhat weaker in an NJL model with  $\Delta = 25$  MeV. It turns out that this ten-

dency continues with increasing coupling strength: For  $H = 3/4 G$  we find that both transitions take place at approximately the same chemical potential, while for  $H = G$  the critical chemical potential for entering the gapless regime is even shifted upwards by almost 10 MeV in the kaon condensed phase. Partially, this can be attributed to the fact that the selfconsistently calculated strange quark mass in the CFLK<sup>0</sup> phase is a few percent larger than in the CFL phase, so that the rotation into the kaon condensed phase reduces the stress not as much as for a constant mass. But even if we take the mass ratio out, there remains a discrepancy. This indicates that there are higher-order effects which have been neglected in the effective theory approach, but become important at stronger couplings.

We would like to note that the numerical solution of the coupled gap equations (20) together with the neutrality conditions (21) turned out to be extremely difficult to obtain in the gCFLK<sup>0</sup> regime. As obvious from the behavior of  $\mu_Q$  at  $T = 0$ , an extrapolation of the solutions from the gapped regime to the gapless regime does not work. Formally, this is related to the fact that, whereas for the gapped solutions the thermodynamic potential at

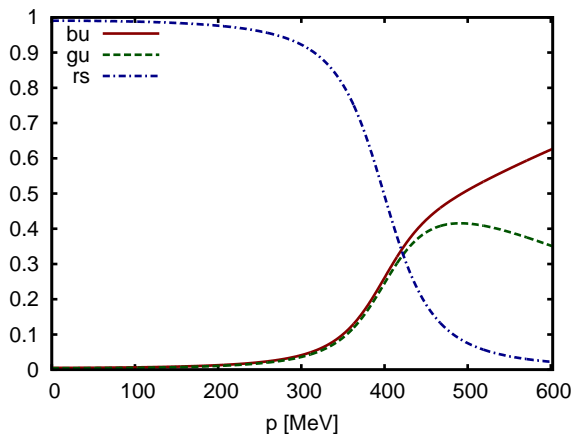


FIG. 7: Composition of the gapless  $\tilde{Q} = 1$  mode in the CFLK<sup>0</sup> phase for  $H = 3/4 G$  at  $\mu = 450$  MeV and  $T = 0$  (cf. Fig. 6, lower left panel). Shown are the squared coefficients of the color-flavor components of the eigenfunctions as functions of the three-momentum.

fixed chemical potentials is a minimum with respect to the various condensates, for the gapless solutions it is a maximum with respect to  $\Delta_{55}^{(s)}$ ,  $\Delta_{52}^{(p)}$  and  $\phi_s$ . At the unpairing line, these minima and maxima merge, and the solutions correspond to inflection points in these parameters.<sup>3</sup> As a consequence, a small variation of the chemical potential can easily lead to a situation, where the solutions of the gap equations disappear completely. Obviously, that makes an iterative solution of the problem in this regime practically impossible.

Since the gapless solutions are very close to the unpairing line, these difficulties are hard to avoid in realistic cases. We have therefore followed the idea of Ref. [17] and introduced additional independent “flavors” of electrons. Then, in order to neutralize the extra negative charge of these electrons, a larger blocking region is needed, so that the gapless solutions move away from the unpairing line and the solutions are easier to find. The resulting dispersion relation of the gapless mode with 250 electron flavors at  $T = 0$  and  $\mu = 450$  MeV is indicated by the green dashed line in Fig. 8. We see that this mode has a blocking region of about 0.5 MeV. For comparison we also show the solution for a world without electrons (red solid line). In this case, there are no negative particles which could neutralize the positive charge of unpaired up quarks. Therefore the size of the blocking region must vanish, i.e., the solution is exactly located on the unpairing line. In this case it can be found coming from the gapped regime.

On the scale of Fig. 6, the two cases shown in Fig. 8 would be indistinguishable and, hence, indistinguishable from the real case with one electron flavor. We also found

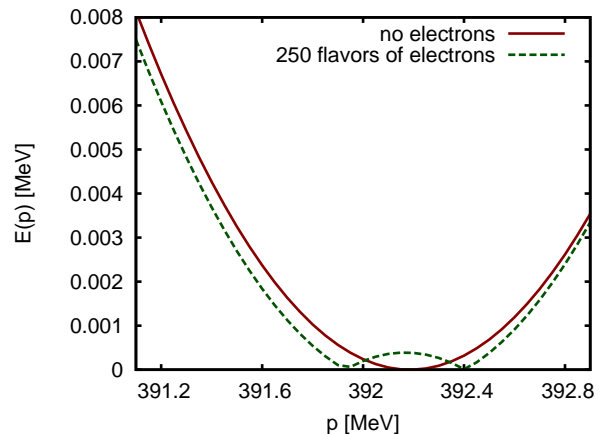


FIG. 8: Dispersion relation of the gapless  $\tilde{Q} = 1$  mode in the CFLK<sup>0</sup> phase at  $\mu = 450$  MeV and  $T = 0$  for  $H = 3/4 G$ . Shown are the neutral solutions in a world with no electrons (red solid line) and in a world with 250 independent electron species (green dashed line). The solution in the real world with one electron species would be very close to the solid line, but qualitatively look like the dashed line, with a tiny blocking region.

that the solutions for the gap parameters, masses, and chemical potentials obtained with 250 or no electron flavors differ only little. The calculation with 250 electron flavors in Fig. 8 mainly serves as an example to prove that gapless CFLK<sup>0</sup> solutions with a finite blocking region indeed exist. Otherwise, of course, the solutions without electrons should be closer to the realistic case. For most practical purposes, we can therefore well approximate the latter by a calculation without electrons. In fact, this is what we have done in Figs. 6 and 7, and in Fig. 4 for  $\mu_Q$  at  $T = 0$ . However, we repeat that the solutions for 250 electron flavors and, hence, for one electron flavor would look the same.

Finally, we want to comment on the role of a finite electron mass  $m_e = 511$  keV, which we have neglected so far. Since  $T \ll m_e$  in the gCFLK<sup>0</sup> phase, this is only justified in the regime where  $|\mu_Q| \gg m_e$ . As we can see in Fig. 4, this condition is fulfilled in the major part of the gCFLK<sup>0</sup> phase. In particular, the existence of the gCFLK<sup>0</sup> phase is not precluded by the electron mass. Of course,  $m_e$  does have a quantitative effect near the threshold to the gapped regime and also on the threshold itself. We recall that, because of  $\tilde{Q}$  neutrality, color neutral quark matter is automatically electrically neutral in the gapped CFLK<sup>0</sup> phase at  $T = 0$ . Therefore no electrons are admitted in the gapped regime, because they would spoil the overall neutrality. However, for nonzero  $m_e$  this does no longer force  $\mu_Q$  to vanish, but any  $|\mu_Q| < m_e$  is allowed. As a consequence, the system can stay in the gapped phase until the unpairing line, which in the relevant regime is given by the red solid line in the lower part of Fig. 4, crosses the line  $\mu_Q = -m_e$ . This shifts the threshold to the gapless phase downwards in  $\mu$  by about 0.4 MeV.

<sup>3</sup> This was also found in Ref.[17] for  $\Delta_{55}^{(s)}$  in the gCFL phase.

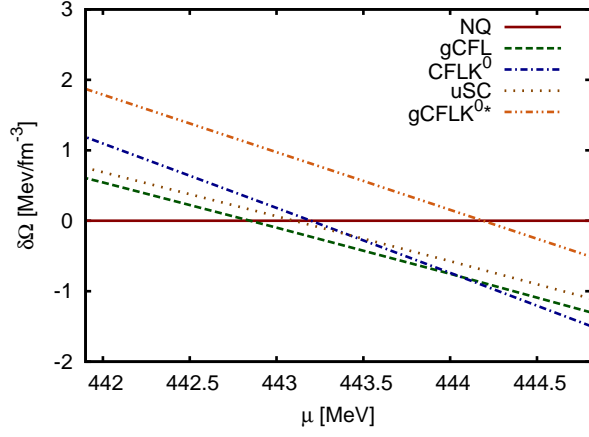


FIG. 9: The free energy of different solutions relative to the normal phase,  $\delta\Omega(T, \mu) = \Omega(T, \mu) - \Omega_{NQ}(T, \mu)$ , for  $H = 3/4 G$  and  $T = 0.5$  MeV as a function of  $\mu$ .

### C. The gCFL window between normal and CFLK<sup>0</sup> phase

We have seen in Figs. 2 and 3 that large parts of the CFL or gCFL phase at not too high temperatures are replaced by the CFLK<sup>0</sup> phase when pseudoscalar condensates are taken into account [52]. As argued in the Introduction, the  $K^0$  condensate reduces the number of strange quarks, which is favorable at “moderate” densities, where the strange quark mass cannot be neglected [33, 34]. Eventually, at very high chemical potentials, the CFL phase should be the most favored phase, but this happens far beyond the range of applicability of our model, which is limited by the cutoff. From this perspective it appears somewhat surprising that for  $H = 3/4 G$  the gCFL phase survives in a small window at the lower- $\mu$  end of the CFLK<sup>0</sup> phase and low temperatures, see Fig. 2. This result is also at variance with Ref. [52] where a uSC phase was found in this regime.

Our result is illustrated by Fig. 9, where the free energy of different solutions relative to the normal phase,  $\delta\Omega = \Omega - \Omega_{NQ}$ , at  $T = 0.5$  MeV is displayed against  $\mu$  in the interesting regime. While the normal phase and the CFLK<sup>0</sup> phase have the lowest free energy at low or high chemical potential, respectively, we see that there is indeed a small intermediate regime where the gCFL phase is favored. The uSC phase, on the other hand, is never favored.

We have mentioned earlier that for low enough chemical potentials, effective field theories predict the existence of CFLK<sup>0</sup> solutions with neutral gapless modes. In the following we will call these solutions ‘gCFLK<sup>0\*</sup> solutions’ for a better distinction from the “ordinary” CFLK<sup>0</sup> solutions with charged gapless modes, as discussed in Sec. III B. In fact, at  $T = 0$ , the gCFLK<sup>0\*</sup> solutions contain both, neutral and charged gapless modes. However, as we have seen for the gCFL phase, the neutral gapless mode should be far more stable at finite temperature.

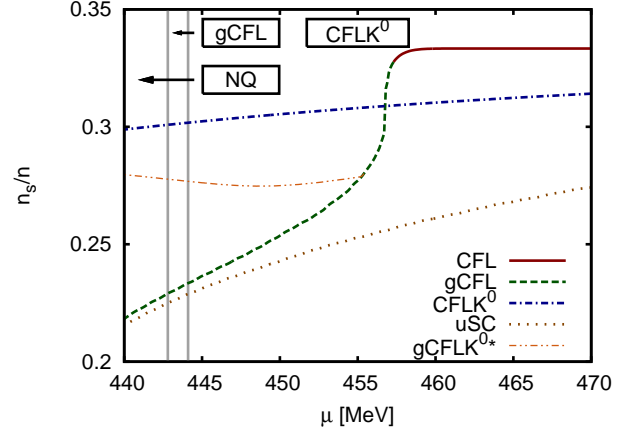


FIG. 10: The fraction  $n_s/n$  of strange quarks in different color superconducting solutions for  $H = 3/4 G$  and  $T = 0.5$  MeV as a function of  $\mu$ . In the boxes it is indicated which phase is realized in the phase diagram (Fig. 2).

In Ref. [39] it was found that at  $T = 0$  the gCFLK<sup>0\*</sup> phase is reached from the ordinary gCFLK<sup>0</sup> phase in a first-order phase transition, where the condensate  $\Delta_{77}^{(s)}$  drops substantially. This is not very different from our CFLK<sup>0</sup>  $\rightarrow$  gCFL phase transition, which is also first order and accompanied by a strong drop of  $\Delta_{77}^{(s)}$ . In fact, the authors of Ref. [39] found that near the phase transition the free energy of the gCFLK<sup>0\*</sup> phase is very close to the free energy of the gCFL phase, so that the result that the former is favored is not very robust.

We have therefore searched for gCFLK<sup>0\*</sup> solutions in this regime. To that end, we have rotated the gCFL solution into the  $K^0$  direction and used the resulting gap parameters as starting values for the iterative solution of the coupled gap equations and neutrality conditions. In this way, we indeed found gCFLK<sup>0\*</sup> solutions, but they turned out not to be favored. For  $T = 0.5$  MeV, this is shown in Fig. 9 as well.

In order to shed some light on these results, we compare the fraction of strange quarks in the various solutions. This is shown in Fig. 10. In the fully gapped CFL phase at zero temperature  $n_s/n = 1/3$ , due to the absence of electrons [60]. At  $T = 0.5$  MeV, this does not hold exactly. Nevertheless, as one can see in the figure,  $n_s/n$  is still very close to one third (solid line). Below  $\mu = 457.1$  MeV the CFL solution becomes gapless (dashed line). Near this point the strange quark fraction drops very steeply with decreasing chemical potential and then approaches smoothly the uSC value (dotted).

The fraction of strange quarks in the CFLK<sup>0</sup> solution is indicated by the dash-dotted line. As expected, the  $K^0$  condensation leads to a reduction of the strangeness content as compared to the fully gapped CFL solution. However, when going to lower chemical potentials,  $n_s/n$  decreases only mildly and is therefore considerably larger than the value in the gCFL solution. From this point of view, it is less surprising that the gCFL solution even-

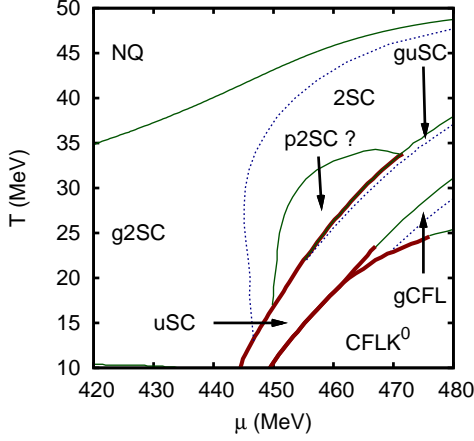


FIG. 11: Detail of the phase diagram for  $H = 3/4 G$ . In contrast to Fig. 2 we have also indicated the region where we numerically find the p2SC phase to be favored.

tually gets favored. Of course, the strangeness content is only one aspect. The reduction of strangeness in the gCFL phase is related to the breaking of pairs and, thus, comes together with a reduction of the pairing energy. As a result, the CFLK<sup>0</sup> phase persists to rather low chemical potentials and the actual phase structure strongly depends on details of the interaction.

For completeness we also show the strangeness fraction in the gCFLK<sup>0\*</sup> solution (dash-double dotted line). This solution only exists below  $\mu = 455.3$  MeV, where it diverges from the gCFL solution by developing pseudoscalar condensates. At lower  $\mu$  it approaches the gapped CFLK<sup>0</sup> solution, and we have strong indications that these solutions eventually join. However, the numerical analysis becomes rather difficult in this regime and, since both solutions are disfavored anyway, we did not make much effort to work this out more carefully.

#### D. The p2SC phase

As mentioned in Sec. III A, we find numerically that the 2SC phase gets partially replaced by a p2SC phase when pseudoscalar condensates are taken into account, see Fig. 11. This was first observed in Ref. [52]. It was found there that in those regions where the p2SC phase is favored, the free energy gain compared with the 2SC solution is very small, less than 1 keV/fm<sup>3</sup>. It was also noted that the p2SC solution is connected to the corresponding 2SC solution via an axial color transformation,

$$q \rightarrow \exp(i\theta \frac{\lambda_7}{2} \gamma_5) q, \quad (23)$$

which partially rotates the condensate  $\Delta_{22}^{(s)}$  into  $\Delta_{25}^{(p)}$ . In this case the condensates in the two phases should be

related as

$$\left(\Delta_{22}^{(s)}\right)_{\text{p2SC}}^2 + \left(\Delta_{25}^{(p)}\right)_{\text{p2SC}}^2 = \left(\Delta_{22}^{(s)}\right)_{\text{2SC}}^2. \quad (24)$$

Indeed, the numerical solutions were found to be in very good agreement with this relation. We confirm all these results.

Nevertheless, the physical significance of this phase is not clear. Unlike the CFLK<sup>0</sup> phase, the p2SC phase is not obviously related to the condensation of a Goldstone mode. In fact, the axial color rotation, Eq. (23), is neither a symmetry of QCD nor of our NJL-model Lagrangian, Eq. (2), not even in the chiral limit. On the other hand, for  $M_u = M_d = 0$  and vanishing color chemical potentials, the mean-field thermodynamic potential is invariant under Eq. (23) if the transformation is restricted to the non-strange sector and only the diquark condensates  $\Delta_{22}^{(s)}$  and  $\Delta_{25}^{(p)}$  are present (see App. A). As a consequence, there is a spurious pseudoscalar Goldstone mode in the 2SC phase at mean field, which is related to the spontaneous breaking of this accidental symmetry by  $\Delta_{22}^{(s)}$ . This suggests that the p2SC phase is an artifact of the mean-field approximation.

Yet, the accidental symmetry does not explain, why the partial rotation of  $\Delta_{22}^{(s)}$  into  $\Delta_{25}^{(p)}$  becomes favored in a certain regime, when we turn to the physical case with nonvanishing up and down quark masses and color chemical potentials. In this context, it is quite instructive to make a comparison with the case of an ordinary (vector) SU(3) color rotation,

$$q \rightarrow \exp(i\theta_a \frac{\lambda_a}{2}) q. \quad (25)$$

It has been observed some time ago that, seemingly, this symmetry can be exploited to neutralize the 2SC phase without introducing color chemical potentials [65]. Thereby  $\Delta_{22}^{(s)}$  is rotated into a different direction in color space, so that equally many red, green, and blue quarks are paired in the condensate. As a consequence, the color charge densities  $n_3$  and  $n_8$  vanish. Moreover, since no color chemical potentials are needed, the resulting state has a lower free energy than the standard neutral 2SC phase with nonvanishing  $\mu_8$ . However, as discussed in Ref. [63], this result is not correct if the NJL model is taken as a model for QCD: A colored state can of course not be neutralized by a color rotation. The color charge is just rotated into a different direction, and instead of  $n_8$  one finds nonvanishing off-diagonal color charge densities  $n_a = \langle q^\dagger \lambda_a q \rangle$  with  $a = 1, 4, 6$  [63]. In QCD, these color charge densities couple to the corresponding gluon fields  $A_a^0$ , which then neutralize the system for all color components. In NJL-type models, where no gluons are present, this must be mimicked by introducing the corresponding (off-diagonal) color chemical potentials. Using these color chemical potentials to remove all (diagonal and off-diagonal) color charge densities, the resulting state is completely equivalent to the standard 2SC phase,

neutralized by  $\mu_8$ . In particular it is no longer energetically favored.

Coming back to our original problem, the situation is quite similar: When we apply the axial color transformation, Eq. (23), to the color non-neutral 2SC phase, the  $n_8$  color charge becomes reduced. However, unlike in the case discussed above, it does not completely reappear in other components  $n_a$ . Instead, the transformation gives rise to a non vanishing *axial* color density,

$$n_a^{(5)} = \langle q^\dagger \gamma_5 \lambda_a q \rangle. \quad (26)$$

To be precise, one finds

$$\begin{aligned} n_8|_{\text{p2SC}} &= \frac{1}{4}(1 + 3 \cos \theta) n_8|_{\text{2SC}}, \\ n_3|_{\text{p2SC}} &= \frac{\sqrt{3}}{4}(1 - \cos \theta) n_8|_{\text{2SC}}, \\ n_6^{(5)}|_{\text{p2SC}} &= -\frac{\sqrt{3}}{2} \sin \theta n_8|_{\text{2SC}}. \end{aligned} \quad (27)$$

Since the sum  $\sum_a (n_a^2 + n_a^{(5)2})$  is conserved in the transformation, the color charge remaining in the vector components gets reduced. Hence, since only the vector color densities  $n_a$  are required to vanish, the rotated solution can be neutralized more easily. This favors the p2SC phase, whereas on the other hand it is disfavored by the nonvanishing up and down quark masses, which break the spurious axial color symmetry explicitly. The fact that the p2SC phase only appears in a certain region of the phase diagram could thus be explained by the interplay of these opposite effects.

As shown in Fig. 12, we indeed find a nonvanishing  $n_6^{(5)}$  in the p2SC phase. Since in QCD there are no “axial gluons”, which could couple to these axial color charges, there is in principle no need to remove them by introducing corresponding “axial color chemical potentials”. In this sense the axial color transformation would be a legitimate way to reduce the free energy of the system. On the other hand, as we have seen before, it is only an accidental (approximate) symmetry of the mean-field thermodynamic potential. It is therefore unlikely that this mechanism works beyond mean field, i.e., the p2SC phase is most likely a model artifact.

Finally, we note that our numerical CFLK<sup>0</sup> solutions have a small axial color charge density, too. Although, unlike in the p2SC phase, the Goldstone modes which condense in the CFLK<sup>0</sup> phase have a well-founded physical basis, this could be a model artifact as well. As already noticed in Ref. [50], the solutions of the gap equations for the scalar and pseudoscalar diquark condensates in the CFLK<sup>0</sup> phase are more similar to an axial color rotation than to an axial flavor rotation of the CFL solutions. On the other hand, both transformations lead to the same result in the chiral limit, i.e., the difference is a higher-order correction in the quark mass. Hence, even if the preference of the axial color rotation was again a model artifact, this would be only a small effect on top of the real physical origin of the CFLK<sup>0</sup> phase.

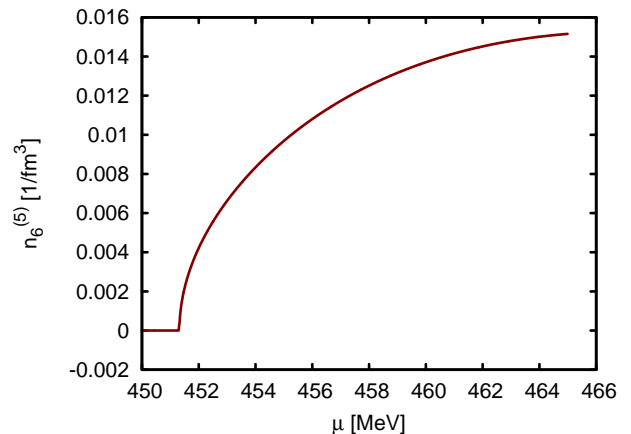


FIG. 12: The axial color density  $n_6^{(5)}$  for  $H = 3/4 G$  at  $T = 25$  MeV as a function of  $\mu$ . The values are nonzero in the p2SC phase and smoothly go to zero at the second-order phase transition to the 2SC phase at  $\mu = 451.3$  MeV.

#### IV. SUMMARY AND CONCLUSIONS

In this paper we have reanalyzed the phase structure of homogeneous electrically and color neutral quark matter within an NJL-type model. Both, quark-antiquark condensates and diquark condensates have been taken into account in order to describe dynamical mass generation and color superconductivity on the same footing. The main focus was on the role of pseudoscalar diquark condensates, which allow for the possibility of kaon condensation in the CFL phase.

A similar investigation was already performed some time ago in Ref. [52]. We confirm the main result that the CFLK<sup>0</sup> phase replaces major parts of the CFL phase in the phenomenologically interesting regime. Numerically, we also confirm that there are regions where a so-called p2SC phase is favored, i.e., a two-flavor superconducting phase with pseudoscalar condensates. We have argued, however, that this is most likely a model artifact.

Our main result is the existence of a gapped CFLK<sup>0</sup> phase at small enough chemical potential and very low temperature,  $T \ll 10$  keV. This is in contrast to Ref. [52], where it was claimed that the entire CFLK<sup>0</sup> phase is completely gapped. The smallness of the critical temperature of the gapless region is due to the fact that the mode contains quarks with nonvanishing  $\tilde{Q}$  charge. Like in the case of the  $bu - rs$  mode in the gCFL phase [17], this keeps the system close to the unpairing line and, even at  $T = 0$ , the blocking region stays very small. A small increase of the temperature is then sufficient to restore the gap by Fermi smearing.

At  $T = 0$ , our results are in qualitative agreement with effective field theory, which predicts that the first gapless mode the CFLK<sup>0</sup> phase is charged [37–39]. However, as also observed in Ref. [51], there are quantitative differences. For large coupling constants we even find that the CFLK<sup>0</sup> phase gets gapless at larger chemical potentials



than the CFL phase. We also identified CFLK<sup>0</sup> solutions with neutral gapless modes, which have been predicted within effective field theory as well [37–39]. In our analysis, however, these solutions were never favored.

It is well known that the gapless 2SC and CFL phases at low temperatures suffer from chromomagnetic instabilities, signalling that these phases are not the true ground state. For the gCFLK<sup>0</sup> phase with charged gapless modes it was shown in Ref. [39] that all Meissner masses are real. Nevertheless the authors found a weak instability with respect to the spontaneous formation of a Goldstone-boson current, corresponding to a  $p$ -wave kaon condensate [40, 41]. This, and the fact that, at least for some parameters, we still found regions where the gCFL phase is favored lead us to the conclusion that the phases indicated in Figs. 2 and 3 do not always represent the true ground state of the system. Most promising candidates for improvements are inhomogeneous or anisotropic phases. This includes the above-mentioned  $p$ -wave kaon condensates as well a crystalline color superconducting phases [24–32].

### Acknowledgments

We thank H. Warringa for useful discussions and M. Alford, C. Kouvaris, V. Kleinhaus, K. Rajagopal, and F. Sandin for valuable information about their numerical gCFL solutions. The work of H.B. was supported by the Helmholtz International Center for FAIR and by the Helmholtz Graduate School for Hadron and Ion Re-

search. M.B. acknowledges partial support by EMMI.

### Appendix A: Axial color symmetry of the mean-field thermodynamic potential in the (p)2SC phase

In this appendix we show that, for  $M_u = M_d = 0$  and vanishing color chemical potentials, the mean-field thermodynamic potential, Eq. (18), is invariant under the axial color transformation, Eq. (23), if the transformation is restricted to the non-strange sector and only the diquark condensates  $\Delta_{22}^{(s)}$  and  $\Delta_{25}^{(p)}$  are present.

If  $\Delta_{22}^{(s)}$  and  $\Delta_{25}^{(p)}$  are the only non-vanishing diquark condensates, the inverse propagator  $S^{-1}$ , Eq. (16), can be put in a block-diagonal form with four  $6 \times 6$  and six  $2 \times 2$  blocks. The  $6 \times 6$  blocks contain the paired up and down quarks. Since all colors participate in the pairing, these blocks are larger than the corresponding blocks in the 2SC phase, which are  $4 \times 4$  blocks. The  $2 \times 2$  blocks correspond to the (unpaired) strange quarks. Note that for  $M_u = M_d = 0$  and, hence,  $\phi_u = \phi_d = 0$ , the strange sector completely decouples from the non-strange sector in the (p)2SC phase. Therefore, since we have restricted the axial color transformation to the non-strange sector, the  $2 \times 2$  blocks will not be affected by the transformation. Therefore we focus only on the  $6 \times 6$  blocks.

Without loss of generality, we may choose the three-momentum of the quark to be parallel to the  $z$ -axis, i.e.,  $\vec{p} = p\vec{e}_3$ . For  $M_u = M_d = 0$  and vanishing color chemical potentials the  $6 \times 6$  matrices then take the form

$$\left(S_{u_b-d_r-u_g}^{\pm}\right)^{-1} = \begin{pmatrix} p_0 \pm \mu_u & -p & -\Delta_{25}^{(p)} & 0 & 0 & 0 \\ -p & p_0 \pm \mu_u & 0 & \Delta_{25}^{(p)} & 0 & 0 \\ -\Delta_{25}^{(p)} & 0 & p_0 \mp \mu_d & p & 0 & \mp \Delta_{22}^{(s)} \\ 0 & \Delta_{25}^{(p)} & -p & p_0 \mp \mu_d & \pm \Delta_{22}^{(s)} & 0 \\ 0 & 0 & 0 & \pm \Delta_{22}^{(s)} & p_0 \pm \mu_u & -p \\ 0 & 0 & \mp \Delta_{22}^{(s)} & 0 & -p & p_0 \pm \mu_u \end{pmatrix} \quad (\text{A1})$$

and

$$\left(S_{d_b-u_r-d_g}^{\pm}\right)^{-1} = \left[\left(S_{u_b-d_r-u_g}^{\pm}\right)^{-1} \text{ with } u \leftrightarrow d\right]. \quad (\text{A2})$$

Here  $\mu_u$  ( $\mu_d$ ) is the chemical potential for the up (down)

quarks. Taking the determinant, we obtain

$$\begin{aligned} & \det \left[ \left(S_{u_b-d_r-u_g}^{\pm}\right)^{-1} \right] \\ &= \left[ (p_0 \pm \mu_u)^2 + p^2 \right] \\ & \quad \times \left[ ((p_0 \mp \mu_d) \pm p) ((p_0 \pm \mu_u) \mp p) - (\Delta_{22}^{(s)})^2 - (\Delta_{25}^{(p)})^2 \right] \\ & \quad \times \left[ ((p_0 \mp \mu_d) \mp p) ((p_0 \pm \mu_u) \pm p) - (\Delta_{22}^{(s)})^2 - (\Delta_{25}^{(p)})^2 \right] \end{aligned} \quad (\text{A3})$$

and the analogous result for  $\det[(S_{d_b-u_r-d_g}^{\pm})^{-1}]$  with  $\mu_u$  and  $\mu_d$  interchanged.

We see that the determinants and, hence,  $\text{Tr} \ln S^{-1} = \ln \det S^{-1}$  depend only on the sum  $(\Delta_{22}^{(s)})^2 + (\Delta_{25}^{(p)})^2$ , which is invariant under the axial color rotation, cf. Eq. (24). The same is obviously true for  $\mathcal{V}$ , Eq. (15). Consequently, the mean-field thermodynamic potential, Eq. (18), is invariant, too.

Note that it was important that we have restricted ourselves to the limit  $M_u = M_d = 0$ . Otherwise  $\Omega$  would

not be invariant. In particular, we would then have to transform the condensates  $\phi_u$  and  $\phi_d$  as well. For the same reason, we have restricted the transformation to the non-strange sector. Alternatively, we could have considered the case where the strange quark mass vanishes, too. However, this would be a rather poor approximation for the real situation in the (p)2SC phase.

- 
- [1] K. Rajagopal and F. Wilczek, arXiv:hep-ph/0011333.
  - [2] M. G. Alford, Ann. Rev. Nucl. Part. Sci. **51**, 131 (2001) [arXiv:hep-ph/0102047].
  - [3] T. Schäfer, arXiv:hep-ph/0304281.
  - [4] D. H. Rischke, Prog. Part. Nucl. Phys. **52**, 197 (2004) [arXiv:nucl-th/0305030].
  - [5] M. Buballa, Phys. Rept. **407**, 205 (2005) [arXiv:hep-ph/0402234].
  - [6] I. A. Shovkovy, Found. Phys. **35**, 1309 (2005) [arXiv:nucl-th/0410091].
  - [7] M. G. Alford, A. Schmitt, K. Rajagopal and T. Schäfer, Rev. Mod. Phys. **80**, 1455 (2008) [arXiv:0709.4635 [hep-ph]].
  - [8] T. Schäfer, Nucl. Phys. B **575**, 269 (2000) [arXiv:hep-ph/9909574].
  - [9] N. J. Evans, J. Hormuzdiar, S. D. H. Hsu and M. Schwetz, Nucl. Phys. B **581**, 391 (2000) [arXiv:hep-ph/9910313].
  - [10] M. G. Alford, K. Rajagopal and F. Wilczek, Nucl. Phys. B **537**, 443 (1999) [arXiv:hep-ph/9804403].
  - [11] M. G. Alford, K. Rajagopal and F. Wilczek, Phys. Lett. B **422**, 247 (1998) [arXiv:hep-ph/9711395].
  - [12] R. Rapp, T. Schäfer, E. V. Shuryak and M. Velkovsky, Phys. Rev. Lett. **81**, 53 (1998) [arXiv:hep-ph/9711396].
  - [13] G. Sarma, J. Phys. Chem. Solids **24**, 1029 (1963)
  - [14] I. Shovkovy and M. Huang, Phys. Lett. B **564**, 205 (2003) [arXiv:hep-ph/0302142].
  - [15] M. Huang and I. Shovkovy, Nucl. Phys. A **729**, 835 (2003) [arXiv:hep-ph/0307273].
  - [16] M. Alford, C. Kouvaris and K. Rajagopal, Phys. Rev. Lett. **92**, 222001 (2004) [arXiv:hep-ph/0311286].
  - [17] M. Alford, C. Kouvaris and K. Rajagopal, Phys. Rev. D **71**, 054009 (2005) [arXiv:hep-ph/0406137].
  - [18] M. Huang and I. A. Shovkovy, Phys. Rev. D **70**, 051501 (2004) [arXiv:hep-ph/0407049].
  - [19] R. Casalbuoni, R. Gatto, M. Mannarelli, G. Nardulli and M. Ruggieri, Phys. Lett. B **605**, 362 (2005); Erratum-ibid. B **615**, 297 (2005) [arXiv:hep-ph/0410401].
  - [20] K. Fukushima, Phys. Rev. D **72**, 074002 (2005) [arXiv:hep-ph/0506080].
  - [21] P. F. Bedaque, Nucl. Phys. A **697**, 569 (2002) [arXiv:hep-ph/9910247].
  - [22] F. Neumann, M. Buballa and M. Oertel, Nucl. Phys. A **714**, 481 (2003) [arXiv:hep-ph/0210078].
  - [23] S. Reddy and G. Rupak, Phys. Rev. C **71**, 025201 (2005) [arXiv:nucl-th/0405054].
  - [24] M. G. Alford, J. A. Bowers and K. Rajagopal, Phys. Rev. D **63**, 074016 (2001) [arXiv:hep-ph/0008208].
  - [25] J. A. Bowers and K. Rajagopal, Phys. Rev. D **66**, 065002 (2002) [arXiv:hep-ph/0204079].
  - [26] R. Casalbuoni and G. Nardulli, Rev. Mod. Phys. **76**, 263 (2004) [arXiv:hep-ph/0305069].
  - [27] I. Giannakis and H. C. Ren, Phys. Lett. B **611**, 137 (2005) [arXiv:hep-ph/0412015]; I. Giannakis, D. f. Hou and H. C. Ren, Phys. Lett. B **631**, 16 (2005) [arXiv:hep-ph/0507306].
  - [28] R. Casalbuoni, R. Gatto, N. Ippolito, G. Nardulli and M. Ruggieri, Phys. Lett. B **627**, 89 (2005); Erratum-ibid. B **634**, 565 (2006) [arXiv:hep-ph/0507247].
  - [29] M. Mannarelli, K. Rajagopal and R. Sharma, Phys. Rev. D **73**, 114012 (2006) [arXiv:hep-ph/0603076].
  - [30] K. Rajagopal and R. Sharma, Phys. Rev. D **74**, 094019 (2006) [arXiv:hep-ph/0605316].
  - [31] D. Nickel and M. Buballa, Phys. Rev. D **79**, 054009 (2009) [arXiv:0811.2400 [hep-ph]].
  - [32] A. Sedrakian and D. H. Rischke, Phys. Rev. D **80** (2009) 074022 [arXiv:0907.1260 [nucl-th]].
  - [33] T. Schäfer, Phys. Rev. Lett. **85**, 5531 (2000).
  - [34] P. F. Bedaque and T. Schäfer, Nucl. Phys. A **697**, 802 (2002) [arXiv:hep-ph/0105150].
  - [35] D. B. Kaplan and S. Reddy, Phys. Rev. D **65**, 054042 (2002).
  - [36] D. T. Son and M. A. Stephanov, Phys. Rev. D **61**, 074012 (2000) [arXiv:hep-ph/9910491]; erratum ibid D **62**, 059902 (2000) [arXiv:hep-ph/0004095].
  - [37] A. Kryjevski and T. Schäfer, Phys. Lett. B **606**, 52 (2005) [arXiv:hep-ph/0407329].
  - [38] A. Kryjevski and D. Yamada, Phys. Rev. D **71**, 014011 (2005) [arXiv:hep-ph/0407350].
  - [39] A. Gerhold, T. Schäfer and A. Kryjevski, Phys. Rev. D **75**, 054012 (2007) [arXiv:hep-ph/0612181].
  - [40] A. Kryjevski, Phys. Rev. D **77**, 014018 (2008) [arXiv:hep-ph/0508180].
  - [41] T. Schäfer, Phys. Rev. Lett. **96**, 012305 (2006) [arXiv:hep-ph/0508190].
  - [42] D. Nickel, J. Wambach and R. Alkofer, Phys. Rev. D **73**, 114028 (2006) [arXiv:hep-ph/0603163].
  - [43] D. Nickel, R. Alkofer and J. Wambach, Phys. Rev. D **74**, 114015 (2006) [arXiv:hep-ph/0609198].
  - [44] F. Marhauser, D. Nickel, M. Buballa and J. Wambach, Phys. Rev. D **75**, 054022 (2007) [arXiv:hep-ph/0612027].
  - [45] D. Nickel, R. Alkofer and J. Wambach, Phys. Rev. D **77**, 114010 (2008) [arXiv:0802.3187 [hep-ph]].
  - [46] S. B. Rüster, V. Werth, M. Buballa, I. A. Shovkovy and D. H. Rischke, Phys. Rev. D **72**, 034004 (2005) [arXiv:hep-ph/0503184].
  - [47] D. Blaschke, S. Fredriksson, H. Grigorian, A. M. Oztas and F. Sandin, Phys. Rev. D **72**, 065020 (2005) [arXiv:hep-ph/0503194].
  - [48] H. Abuki, M. Kitazawa and T. Kunihiro, Phys. Lett. B **615**, 102 (2005) [arXiv:hep-ph/0412382].
  - [49] H. Abuki and T. Kunihiro, Nucl. Phys. A **768**, 118 (2006) [arXiv:hep-ph/0509172].

- [50] M. Buballa, Phys. Lett. B **609**, 57 (2005) [arXiv:hep-ph/0410397].
- [51] M. M. Forbes, Phys. Rev. D **72**, 094032 (2005) [arXiv:hep-ph/0411001].
- [52] H. J. Warringa, arXiv:hep-ph/0606063.
- [53] G. 't Hooft, Phys. Rev. D **14**, 3432 (1976) [Erratum-ibid. D **18**, 2199 (1978)]. G. 't Hooft, Phys. Rept. **142**, 357 (1986).
- [54] K. Iida, T. Matsuura, M. Tachibana and T. Hatsuda, Phys. Rev. D **71**, 054003 (2005) [arXiv:hep-ph/0411356].
- [55] D. Ebert and K. G. Klimenko, Phys. Rev. D **75**, 045005 (2007) [arXiv:hep-ph/0611385].
- [56] D. Ebert, K. G. Klimenko and V. L. Yudichev, Eur. Phys. J. C **53**, 65 (2008) [arXiv:0705.2666 [hep-ph]].
- [57] V. Kleinhaus, M. Buballa, D. Nickel and M. Oertel, Phys. Rev. D **76**, 074024 (2007) [arXiv:0707.0632 [hep-ph]].
- [58] V. Kleinhaus and M. Buballa, Phys. Rev. D **79**, 014016 (2009) [arXiv:0808.3490 [hep-ph]].
- [59] M. G. Alford, J. Berges and K. Rajagopal, Nucl. Phys. B **571**, 269 (2000) [arXiv:hep-ph/9910254].
- [60] K. Rajagopal and F. Wilczek, Phys. Rev. Lett. **86**, 3492 (2001) [arXiv:hep-ph/0012039].
- [61] A. W. Steiner, S. Reddy and M. Prakash, Phys. Rev. D **66**, 094007 (2002) [arXiv:hep-ph/0205201].
- [62] S. B. Rüster, arXiv:nucl-th/0612090.
- [63] M. Buballa and I. A. Shovkovy, Phys. Rev. D **72**, 097501 (2005) [arXiv:hep-ph/0508197].
- [64] P. Rehberg, S. P. Klevansky and J. Hüfner, Phys. Rev. C **53**, 410 (1996) [arXiv:hep-ph/9506436].
- [65] D. Blaschke, D. Gomez Dumm, A. G. Grunfeld and N. N. Scoccola, arXiv:hep-ph/0507271.